Environ Biol Fish (2024) 107:1137–1153
https://doi.org/10.1007/s10641-024-01608-0

Population structure of the Atlantic angel shark (*Squatina dumeril*) in United States waters of the western North Atlantic Ocean

Andrew T. Fields · William B. Driggers III · Christian M. Jones · David S. Portnoy

Received: 26 June 2024 / Accepted: 23 September 2024 / Published online: 11 October 2024

Abstract While dorsal-ventrally compressed chondrichthyans are among the most imperiled fishes in the world, there is still limited knowledge of the biology of many of these species, even in well-studied ocean basins. In the western North Atlantic Ocean, the population structure of the Atlantic angel shark (*Squatina dumeril*) is not fully understood; therefore, the portioning of genetic variation was assessed among individuals caught along the east coast of the United States (Atlantic) and on the northern Gulf of Mexico (Gulf) using reduced representation genomics and mitochondrial sequencing. Three distinct groups were delineated with nuclear data, the Atlantic, the eastern Gulf, and the western Gulf, along boundaries described by previous research. Mitochondrial data only resolved two groups, with the western Gulf separated from the eastern Gulf and Atlantic combined. Demographic modeling suggested that the Atlantic population separated from a single Gulf population which subsequently split into eastern and western populations. Additionally, there was evidence that adjacent populations experienced gene flow after splitting, which may explain the incongruence between results based on nuclear and mtCR data. Correlations between environmental variables and allele frequencies at 873 loci indicated potential local adaptation. Therefore, the preservation of all three groups is necessary for the conservation of long-term adaptive variation important for species persistence.

Keywords Angel shark · Squatinidae · Genetic demography · Stock structure

Supplementary Information The online version contains supplementary material available at https://doi.org/10.1007/s10641-024-01608-0.

A. T. Fields (✉) · D. S. Portnoy (✉)
Marine Genomics Laboratory, Department of Life Sciences, Texas A&M University—Corpus Christi, 6300 Ocean Drive, Corpus Christi, TX 78412, USA
e-mail: andrew.fields.biologist@gmail.com

D. S. Portnoy
e-mail: David.Portnoy@tamucc.edu

W. B. Driggers III · C. M. Jones
Southeast Fisheries Science Center, National Marine Fisheries Service, National Oceanic and Atmospheric Administration, P.O. Drawer 1207, Pascagoula, MS 39567, USA

Introduction

Fisheries-induced mortality of elasmobranchs has led to population declines across the globe (Ferretti et al. 2010; Worm et al. 2013). Some of the most imperiled species are rays and ray-like sharks, such as guitarfish and angel sharks (Dulvy et al. 2014). For angel sharks (family, Squatinidae; genus, *Squatina*), concerns about sustainability relate to long generation times and low fecundities (Lawson et al. 2020) paired with harvest-related mortality, either through directed or incidental catch (e.g., Vecchione 1987; Leet et al.

2001; Villwock and Vooren 2003; Scandol et al. 2008; Raoult et al. 2017). Compounding the problem, these species are data-limited, and aspects of their biology are not well-understood, even in some of the most well-regulated waters. This includes limitations on the knowledge of angel shark stock structure (Ellis et al. 2021), constraining the ability to properly assess and manage stocks (Cadrin et al. 2014).

In the past couple of decades, research has increasingly focused on species in the genus *Squatina*, collectively known as angel sharks. Of the 24 angel shark species currently considered valid, four species were described in the past 10 years, and three additional species were described in 2007–2008 (Last and White 2008; Acero et al. 2016; Vaz and Carvalho 2018; Long et al. 2021; Weigmann et al. 2023). Four of these newly described species were in waters associated with the Coral Triangle and Australia, two were described from the western Atlantic Ocean, and the remaining one was described off eastern Africa. Among extant species, the range of many overlap including four species around Australia (*S. albipunctata*, *S. australis*, *S. pseudocellata*, and *S. tergocellata*), four species in the northwestern Pacific (*S. formosa*, *S. japonica*, *S. nebulosi*, and *S. tergocellatoides*), three species in the Mediterranean and eastern Atlantic Ocean (*S. aculeata*, *S. oculata*, and *S. squatina*), and four species along eastern Central and South America (*S. argentina*, *S. guggenheim*, *S. occulta*, and *S. varii*). A recent study also suggests range overlap may be found along the southeastern Pacific (Cañedo-Apolaya et al. 2021), though it has not been formally described. Three other angel shark species (*S. caillieti*, *S. legnota*, and *S. mapama*) are not reported to have overlapping ranges with other species; however, because they have recently been described and their full range is unknown, further investigation is required to determine if this is true.

In fact, very few species in the family Squatinidae actually do not show some overlap with congeners, including *S. californica* found in the eastern Pacific Ocean (Gaida 1997; Cañedo-Apolaya et al. 2021), *S. africana* and *S. leae* both found in the western Indian Ocean, *S. david* in the central western Atlantic, and *S. dumeril* found in northwestern Atlantic Ocean, including the Gulf of Mexico and Caribbean Sea. While research has suggested that three species could be present in the Gulf of Mexico (Castro-Aguirre et al. 2006), those species names (*i.e.*, *S. heteroptera* and *S. mexicana*) are all currently considered synonyms of *S. dumeril* (Fricke et al. 2024). A large portion of the range of *S. dumeril* in U.S. waters of the western North Atlantic Ocean was recently surveyed, and the species was found to have two distinct distributional breaks based on fisheries-independent catch records (Driggers et al. 2018). The first of these breaks separates *S. dumeril* off the east coast of the U.S. (Atlantic) from those in the Gulf of Mexico (Gulf), with the second break found adjacent to the Mississippi Canyon within the Gulf (Driggers et al. 2018). Driggers et al. (2018) also discussed differences in depth distribution among the regions and provided a thorough discussion of the potential for different species to be found in US waters of the western North Atlantic Ocean.

A previous study that characterized the genetic variation of *S. dumeril* in U.S. waters using the mitochondrial control region (mtCR) found a significant difference between the western and eastern Gulf but not between the Atlantic and the eastern Gulf (McMillan 2009). This result is somewhat surprising as the distributional break between the Atlantic and the Gulf seems to be more dramatic than the break within the Gulf (Driggers et al. 2018). Given the discordance between the results of mtCR-based analyses and distributional patterns, and the fact that many angel shark species have recently been discovered due to increased scrutiny, a reassessment of the portioning of genetic variation that considers variation in nuclear-encoded DNA is warranted. Therefore, patterns of genetic variation were assessed in *S. dumeril* in the western North Atlantic using thousands of SNP-containing loci across the genome to look for cryptic diversity and assess population structure. Because *S. dumeril* is currently distributed in areas impacted by recent glacial cycles, demographic history was also modeled using site frequency spectrum analysis.

Materials and methods

Sample collection and nuclear sequencing

Specimens from which tissues were derived were collected during the National Marine Fisheries Service (NMFS), Southeast Fisheries Science Center (SEFSC) trawl survey operations in the northern Gulf

and the Virginia Institute of Marine Science (VIMS), Northeast Area Monitoring and Assessment Program (NEAMAP) trawl survey operations along the U.S. Atlantic Seaboard (Fig. 1) during 2016 and 2017. Tissues from *S. californica* were provided by the University of Kansas (KU# 437, 438) and Scripps Institution of Oceanography (09–296, 11–322). DNA was extracted using Mag-Bind Blood and Tissue DNA kits (Omega Bio-Tek, Norcross, GA), and approximately 1000 ng of high-quality genomic DNA was used in a modified version of double digest restriction-site associated DNA (ddRAD) library preparation method (Peterson et al. 2012). In brief, extractions were digested with restriction enzymes *Eco*RI and *Sph*I, and a barcoded adapter was ligated to *Sph*I restriction sites, while a common adapter was ligated to *Eco*RI restriction sites. Individuals with different barcodes were subsequently pooled, using equimolar quantities of each ligated sample, into two "indexed" libraries consisting of 30 and 39 individuals per index, and size was selected using a Pippin Prep DNA size selection system (Sage Science Inc., Beverly, MA). Fragments were selected using a mean size of 340 bp, with a selection window of ± 37 bp. Illumina flow-cell adapter sequences and index-specific identifiers were added to each index, using 14 cycles of PCR. This process results in every individual having unique combinations of barcode and index sequence, allowing for unequivocal identification after sequencing. Each index was sequenced as part of an Illumina HiSeq 4000 sequence lane at Genewiz (Azenta, South Plainfield, NJ) with technical replicates (duplicated individuals) sequenced across the indices.

Data processing: ddRAD

Raw Illumina HiSeq reads from each individual were demultiplexed using the "process_radtags" function in the software *Stacks* v2.59 (Catchen et al. 2013), and 30 samples, ten from each of the western Gulf, eastern Gulf, and the Atlantic, were used to create a de novo reference of putatively single-copy contigs using the *dDocent* v2.8.7 pipeline (Puritz et al. 2014). From this reference, single nucleotide polymorphisms (SNPs) were identified. Mapped reads were filtered to remove those that were not properly paired, had secondary alignments, and had a quality score below 40. Results were compiled into a variant call file (VCF) file, and variants were filtered using a combination of VCFtools v0.1.14 (Danacek et al. 2011) and custom R, BASH, and Perl scripts to remove artifacts following O'Leary et al. (2018). These filters included

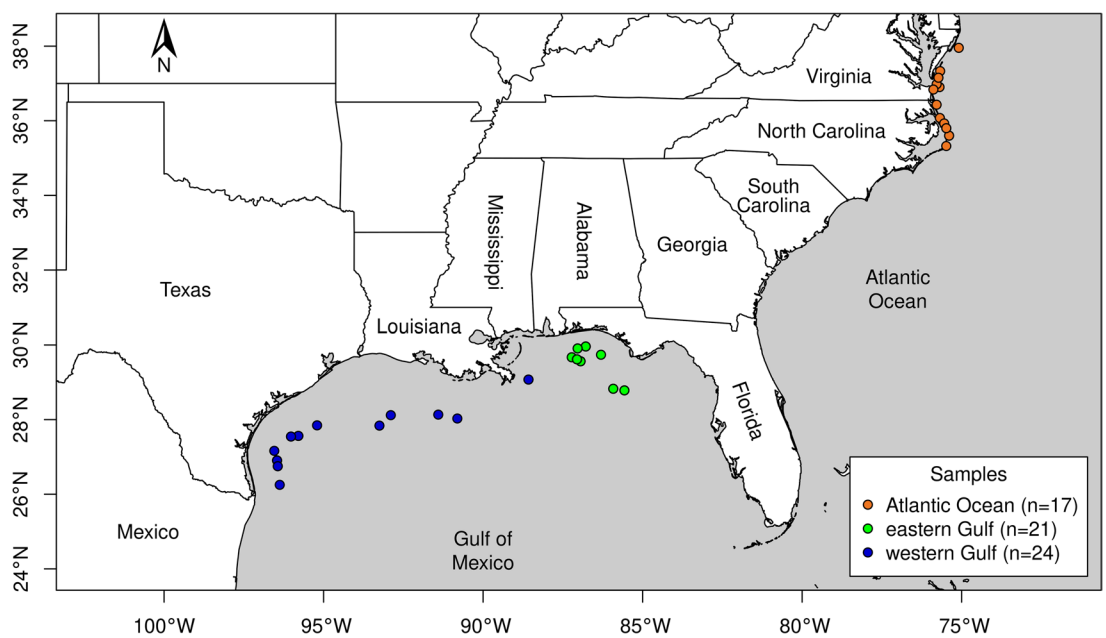

Fig. 1 Distribution of the *S. dumeril* samples analyzed, color-coded by the *k*-means group to which they were assigned with a $K = 3$

removing loci with low average depth, loci with very high average depth, genotypes with low-quality scores, individuals with low average depth, genotypes with highly skewed allelic balance, loci influenced by library effects, and monomorphic loci and loci with high depth variation across the locus. SNPs on the same fragment were then phased into microhaplotypes (hereafter loci) using the *rad_haplotyper* (Willis et al. 2017), and loci that contained more haplotypes within individuals than expected were removed. Singletons and doubletons were filtered more stringently for depth than other alleles, and a minor allele count of 3 was applied. Scripts and further details are available at https://github.com/marinegenomicslab/Fields2024_Angel_Sharks.git.

Analysis: ddRAD

All analyses excluded *S. californica* unless indicated otherwise. Principal component analysis (PCA) and *k*-means clustering ($n = 1$–40) were used to identify the optimal number of groups using the Bayesian Information Criterion (BIC). The groupings with the lowest BIC and adjacent values were compared using discriminant analysis of principal components (DAPC) cross-validation to determine the optimal number of PCs required to achieve the highest reassignment of samples to their respective groups in *adegenet* v2.1.5 (Jombart 2008). Missing data were imputed by using mean allele frequencies.

Loci that deviate from drift-mutation equilibrium can provide a misleading demographic pattern from the major goal of analyses to understand connectivity and historical demography (Funk et al. 2012); therefore, two approaches were used to locate non-neutral loci. First, redundancy analysis (RDA) was used to find loci associated with environmental pressures, which could shape the genetic landscape through selection pressures. Additionally, genetic data were scanned for F_{ST} outliers to find loci with F_{ST} values outside the general distribution and therefore possibly undergoing selection.

Environmental (abiotic) measurements and spatial variables were compared in the genetic data using RDA implemented in the R package *vegan* v2.5–7 (Oksanen et al. 2019). Marine environmental variable data ($n = 916$) were downloaded from two long-term, spatial data sets collated across multiple detection methods which include integrated remote sensing data (e.g., primary productivity, temperature), integrated ship collected data (e.g., nitrogen, phosphorus), and modeled variable such as currents (e.g., max velocity) collected from stationary buoys. The datasets were collected from BIO-ORACLE (Tyberghein et al. 2012) and MARSPEC (Sbrocco and Barber 2013) using the R package sdmpredictors v 0.2.10 (Bosch and Fernandez 2021). The variation in environmental factors at the catch locations was evaluated, and some had no variation, so they were removed. To account for spatial autocorrelation, the minimum in-water distance along a network with a within-region minimum spanning threshold was used to get the distance between each point. Distances between nodes were calculated using the Haversine formula to correct for the Earth's curvature (Sinnott 1984).

Forward stepwise model selection was used to determine which environmental and spatial variables to include in the final RDA model using a modified version of ordiR2step from the R package *vegan* with 999 permutations and a *p*-value for adding in a variable (Pin) of 0.05. To avoid multicollinearity among explanatory variables, a variance inflation factor (VIF) filter was used before adding each variable to the model. If adding an explanatory variable to the model would increase the VIF of any of the variables above 3, the variable was excluded from analysis (Zuur et al. 2010). The loci associated with a given variable were determined by using a partial RDA constrained by all of the factors, except the one being tested, and removing the loci with the highest loading score, in a backward stepwise fashion, until the constrained RDA was no longer significant.

The dataset was screened for loci potentially under selection, referred to as "outliers," with BAYESCAN v2.1 (Foll and Gaggiotti 2008; Fischer et al. 2011) and OUTFLANK (Whitlock and Lotterhos 2015), implemented through the R package *dartR* v1.8.3 (Gruber et al. 2018). For both analyses, individuals were grouped following the results of *k*-means clustering. The BAYESCAN analysis was performed with 30 pilot runs of 5000 iterations and a burn-in of 50,000 iterations before sampling 5000 times at 100 iteration intervals and a prior odds value of 100. In OUTFLANK, the F_{ST} distribution was made by trimming the upper and lower 5%, and the *q*-value was set to 0.1.

Any locus identified as an outlier by either program was categorized as an outlier in subsequent analyses.

All outliers and environmentally associated loci were separated from the "neutral" loci, resulting in three data sets (neutral, outlier, and environmental). A single-level, locus-by-locus AMOVA was used to assess for genetic heterogeneity in each dataset with Arlequin v3.5 (Excoffier and Lischer 2010) with significance determined through 10,000 permutations. Post hoc pairwise comparisons of F_{ST} between groups were performed using Arlequin for all the datasets, with significance determined as above and corrected for multiple comparisons using the Benjamini and Hochberg false discovery rate (BHFDR) method (Benjamini and Hochberg 1995). Because the maximum value that F_{ST} can reach is dependent on background diversity (Meirmans and Hedrick 2011), the maximum value of F_{ST} (F_{MAX}) will often be less than one. To account for this, neutral estimates of F_{ST} were divided by neutral estimates of F_{MAX} to calculate F'_{ST}. Pairwise F_{MAX} was calculated in Arlequin using recoded data in which each group had unique alleles (Meirmans and Hedrick 2011). Estimates of neutral F'_{ST} were compared between each *S. dumeril* group and *S. californica*.

Mean and locus-by-locus expected heterozygosity (H_e) were estimated using Arlequin, and mean and locus-by-locus allelic richness (A_r) also were estimated using the *hierfstat* v 0.5–7 in R (Goudet and Jombart 2020). Within-group diversity measures were compared among groups using a Friedman's rank sum test in the R package *stats* v 3.6.0 (R Core Team 2019), with post hoc pairwise comparisons of significant factors using a paired Wilcoxon's signed-rank tests performed in the R package *coin* 1.4–1 (Hothorn et al. 2006) which adjusts for tied rank values. Significance values were corrected for multiple comparisons using the Benjamini and Hochberg false discovery rate (BHFDR) method (Benjamini and Hochberg 1995).

mtCR sequencing

The mtCR was PCR amplified for 52 individuals using primers designed to amplify the entire mtCR of multiple shark species (Swift et al. 2023). Reactions of 25 µL included 1 µL of DNA, 1X Green GoTaq® Reaction Buffer, 1.5 mM $MgCl_2$, 200 µM dNTPs, 0.2 mM of each primer, and 1 unit of GoTaq® Polymerase (Promega, Madison, WI). Cycling involved an initial denature of 95 °C for 2 min, 35 cycles of 95 °C for 1 min, 54 °C for 1 min, and 72 °C for 1.5 min, with a final elongation phase of 72 °C for 5 min. Amplicons were purified using the Mag Bing Total-Pure NGS (Omega Bio-Tek), and Sanger sequencing was conducted on an ABI 3730 using just the forward primer at Retrogen (San Diego, CA). Sequences were quality trimmed and aligned using CLUSTAL OMEGA (Sievers et al. 2011), and alignments were checked by eye in BioEdit v. 7.2.5 (Hall 1999).

Analysis: mtCR

Homogeneity of variance was assessed using single-level AMOVA with significance determined by permuting individuals among groups 10,000 times in Arlequin. Post hoc estimates of pairwise Φ_{ST} were also calculated in Arlequin with significance calculated as above and corrected for multiple testing using BHFDR. The mutation model for both analyses was selected using the model with the lowest Bayesian Information Criterion (BIC) value, as calculated in JMODELTEST2 v2.1.10 (Darriba et al. 2012). All samples were assigned to groups based on the ddRAD *k*-means clustering. However, three individuals with mtCR data were not present in the final ddRAD dataset, so they were placed in the Atlantic where they were caught. To visualize the relationship of haplotypes, a TCS network was constructed in POPART v1.7 (Clement et al. 2002; Leigh and Bryant 2015) using the groups defined by the ddRAD analysis. Diversity statistics such as the number of SNPs, mean pairwise differences, transition and transversion counts, and nucleotide diversity were estimated with Arlequin for groups defined by *k*-means clustering.

Demographic modeling

One SNP was randomly selected from each neutral locus, and the resulting data set was used to examine historical demography using site frequency spectrum analysis as implemented in MOMENTS v1.0.8 (Jouganous et al. 2017). Five demographic models were considered initially: (1) a null model with all populations splitting at the same time and no migration, (2) a model with the Atlantic separating from an ancestral population before the Gulf split with symmetrical migration, (3) a model with the Atlantic separating from an ancestral population before the Gulf split

with asymmetrical migration, (4) a model where the western Gulf splits from an ancestral population before the Atlantic/eastern Gulf split with symmetrical migration, and (5) a model where the Western Gulf splits from an ancestral population before the Atlantic/eastern Gulf split with asymmetrical migration (Fig. S1). Migration was only allowed between geographically adjacent populations, and population expansion was included within each model except for the null model.

As has been noted by previous researchers, multiple rounds of optimization are required to find the optimal parameters for each demographic model in MOMENTS (Portik et al. 2017; Noskova et al. 2020); therefore, the four-step optimization strategy suggested by Portik et al. (2017) was employed using the default folds and the default maxiters for an optimization round with at least 40 sets of parameters optimized per step. The best parameters from an optimization round were then used to prime the next optimization round. Once two sequential optimization rounds returned the same parameter values, the optimization process was considered complete for that model. The site frequency spectrum (SFS) input into MOMENTS was optimized using easySFS v.0.0.1 and downward projected to the values with the most segregating sites (Gutenkunst et al. 2009; Overcast 2022). Akaike Information Criterion (AIC) was used to select the best demographic model, and confidence intervals for estimated demographic parameters were generated using the Godambe information matrix (Coffman et al. 2016) implemented in MOMENTS.

Results

ddRAD

Fin clips from 69 *S. dumeril* were collected and sequenced across two ddRAD libraries resulting in 504,611 SNPs across 44,651 putative loci. The final assembly parameters were a *c*-value of 0.84, a K_1 of 2, and a K_2 of 2. After filtering, 24,270 SNPs across 7886 SNP-containing loci (henceforth loci) were present in 63 samples, including one Pacific angel shark sample, with an average of 3.08 SNPs and 3.86 alleles per locus.

The minimum BIC score was obtained for $K=1$ (Fig. S2); however, the PCA showed at least two distinct groups: one in the Atlantic and one in the Gulf (Fig. 2). Cross-validation of two and three groups both assigned individuals back to the groups with 100% accuracy, and the three groups corresponded to the Atlantic, the eastern Gulf, and the western Gulf, consistent with known breaks in their distribution (Fig. 1; Driggers et al. 2018). Cross-validation of four groups had a root mean squared error of around 10%. Therefore, the three groups identified by *k*-means clustering were chosen to perform the remaining analyses.

Sea surface temperature (SST) in September and two measures of nitrate levels were significantly associated with genetic variation (Table 1). The three environmental factors explained 7.0% of the genetic variation in the data with 772 loci significantly associated with SST, 127 loci significantly associated with mean nitrate concentration, and 19 loci significantly associated with minimum sea surface nitrate concentration (Fig. S3). Of the 873 loci found to be associated with the three environmental factors, 42 loci were shared between the SST and mean nitrate, one locus shared between the minimum nitrate and SST, and a different locus shared between the two nitrate measures. An additional locus was shared between all the factors. BAYESCAN found 11 loci to have elevated F_{ST} values with positive alphas indicating directional selection. OUTFLANK found ten of the loci recovered by BAYESCAN as well as an additional 17. Three loci were found to be F_{ST} outliers and were associated with environmental variables. This data was split into a neutral dataset of 6973 loci, an environmentally associated (hereafter environmental) dataset of 873, and an F_{ST} outlier (hereafter outlier) dataset of 28 loci for downstream analysis.

Global AMOVAs were significant for all the datasets ($p<0.0001$; Fig. 3), and all pairwise comparisons of F_{ST} for all datasets were also significant (Table 2), though the F_{ST} between the Gulf regions was $>3.5\times$ less than comparisons involving one of the Gulf regions and the Atlantic. Estimates of neutral F'_{ST} between the Gulf and Atlantic samples were an order of magnitude less than between *S. dumeril* and *S. californica* (means of 0.0089 and 0.1389, respectively; Table 3), though due to the limited number of Pacific samples, *p*-values could not be calculated.

Estimates of H_e were significantly heterogeneous ($p<0.01$) for the neutral and outlier datasets, but not the environmental data set. In the neutral data, the

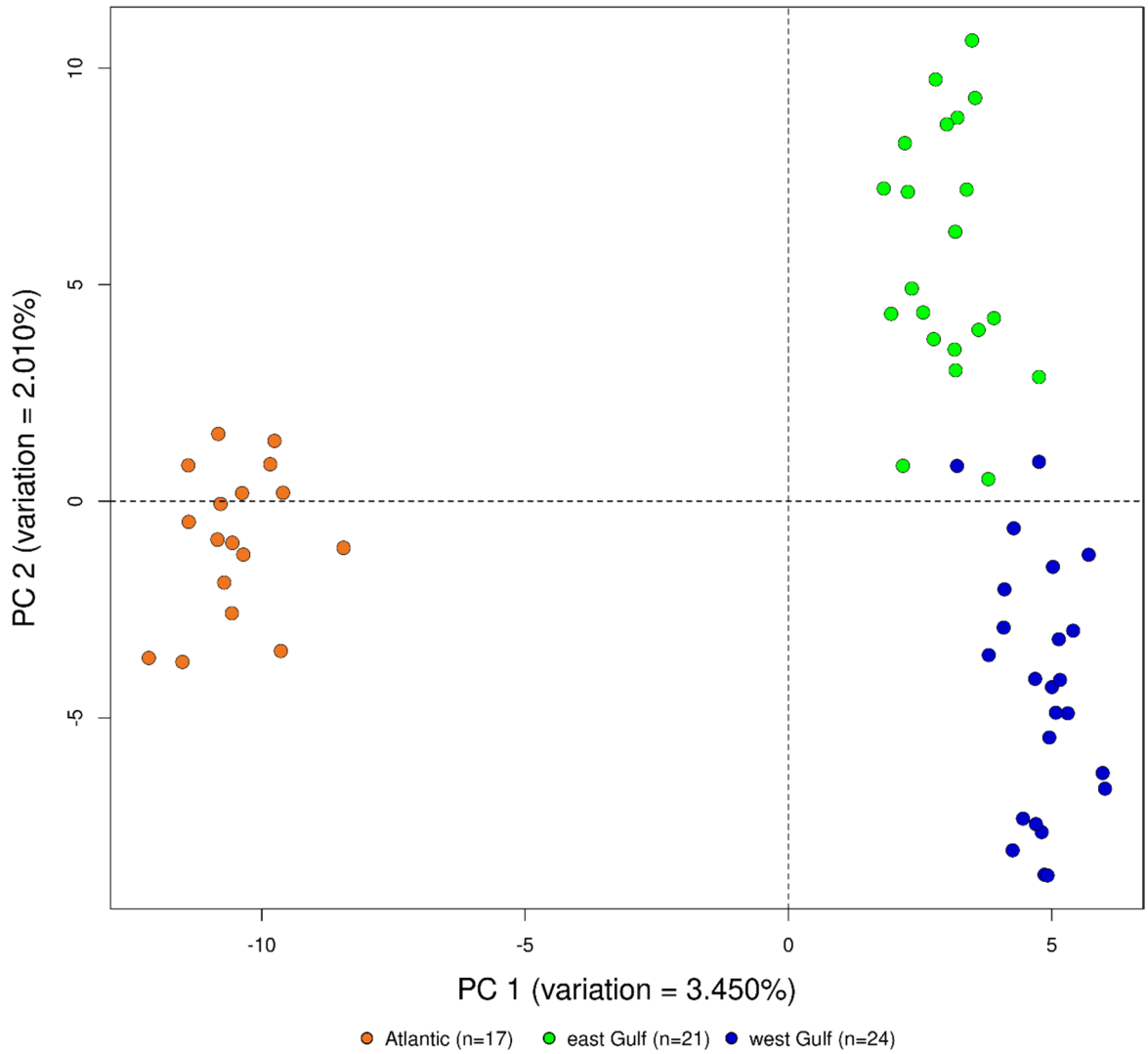

Fig. 2 The first and second axes of a principal components analysis (PCA) of all the data including the amount of variation described by each axis and color-coded by the *k*-means groupings ($K=3$) with orange indicating the Atlantic ($n=17$), green as the eastern Gulf ($n=21$), and blue as the western Gulf ($n=24$)

Table 1 The variance explained, adjusted *R*-squared, and *p*-value for the abiotic factors which significantly explained a portion of the genomic data

RDA factor	Adj *R*-squared	% variation	*p*-value
September sea surface temperature	0.0177	2.57%	< 0.001
Mean annual nitrate	0.0098	1.89%	0.005
Minimum sea surface nitrate concentration	0.0016	1.73%	0.042
Full Model	0.0221	7.02%	< 0.001

The variance in the full model is higher than expected due to the partial collinearity of the variables which increases the variance explained

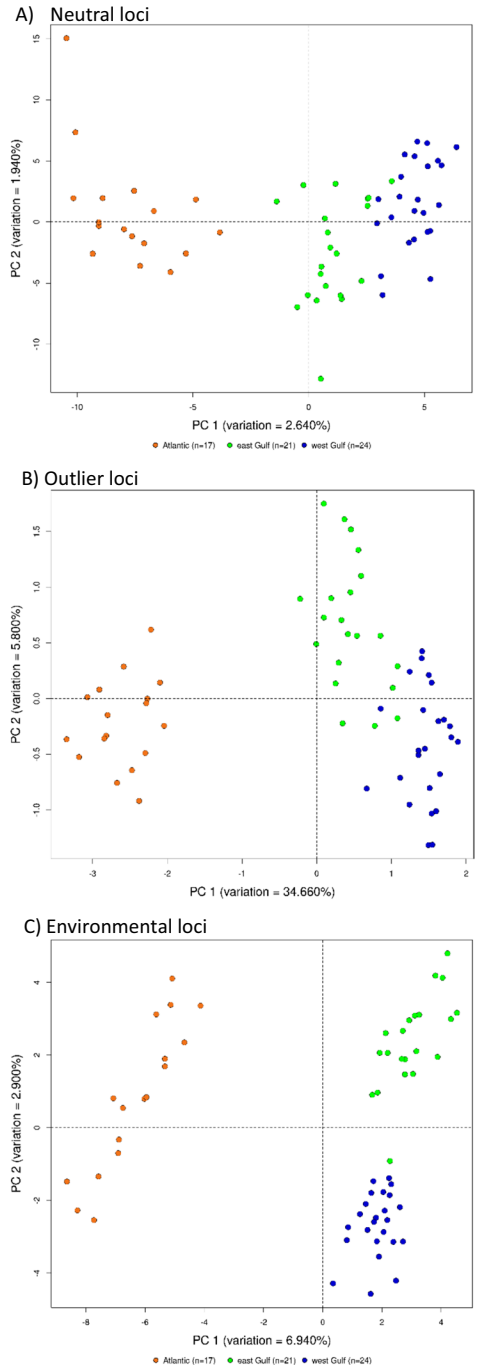

Fig. 3 The first and second axes of a principal components analysis (PCA) of the neutral **A**, F_{ST} outlier **B**, and environmental loci **C** including the amount of variation described by each axis and the global AMOVA values, color-coded by the *k*-means groupings ($K=3$) with orange indicating the Atlantic ($n=17$), green as the eastern Gulf ($n=21$), and blue as the western Gulf ($n=24$)

eastern Gulf had a significantly higher H_e than the other two regions, while in the outlier loci, the western Gulf had significantly lower H_e values (Table 4; Table S2). Estimates of A_r were significantly heterogeneous ($p<0.01$) for the neutral and environmental data sets, but not the outlier data set with the western Gulf having the highest values and the Atlantic having the lowest values.

mtCR

The mtCR of 52 *S. dumeril* was successfully sequenced, and the sequences were trimmed down to a 515 base pair fragment recovered in all individuals (Genbank PP952512—PP952563), which included all of the left domain of the mtCR. Among all of the western North Atlantic samples, 12 polymorphic sites were found, resulting in 17 haplotypes. The eastern Gulf had the highest nucleotide diversity, and the Atlantic had the lowest (Table 5), while the Atlantic had the highest haplotype diversity. The HKY + I model was selected, but because it is not available in ARLEQUIN, the Tamura and Nei mutation model (Tamura and Nei 1993) was used instead. A global AMOVA was significant ($\Phi_{ST}=0.5131$; $p<0.0001$), and estimates of pairwise F_{ST} between the western Gulf and each of the other regions were significant (Table 2). The TCS network indicated two distinct groups with four haplotypes shared between the Atlantic and eastern Gulf samples, though two haplotypes were shared between the eastern Gulf and the western Gulf. No haplotypes were shared between the Atlantic and western Gulf (Fig. 4).

Demographic modeling

The best-supported demographic model contained an initial split between the Atlantic Ocean and an ancestral population in the Gulf of Mexico (Table S1). The ancestral population then proceeded to divide into what is currently the western Gulf of Mexico and the eastern Gulf of Mexico populations (AIC = 4606.96; Fig. S1B). This model indicated population growth from the time of divergence to the present in all populations and that historic symmetrical gene flow between adjacent populations, though gene flow was nearly zero between the original Atlantic and ancestral Gulf populations (Table 6).

Table 2 Pairwise F_{ST} values and their respective p-values for the Φ_{ST} and the p-values for the mitochondrial control region (mtCR) sequencing as well as neutral, environmental, and F_{ST} outlier nuclear ddRAD data

	mtCR		Neutral		Environmental		F_{ST} outlier	
Comparison	F_{ST}	p-value	F_{ST}	p-value	F_{ST}	p-value	F_{ST}	p-value
Atlantic–eastern Gulf	0.0181	0.2449	0.0077	< 0.0001	0. 0758	< 0.0001	0. 2880	< 0.0001
Atlantic–western Gulf	0.6542	< 0.0001	0.0157	< 0.0001	0.0655	< 0.0001	0.4491	< 0.0001
Eastern Gulf–western Gulf	0.5275	< 0.0001	0.0021	0.0001	0.0167	< 0.0001	0.0964	< 0.0001

Table 3 Pairwise F'_{ST} values for the neutral nuclear ddRAD data including the Pacific angel shark

	Atlantic	east Gulf	west Gulf	Pacific
Atlantic	-			
east Gulf	0.0107	-		
west Gulf	0.0218	0.0030	-	
Pacific	0.1473	0.1263	0.1432	-

Table 5 Basic statistics from mtCR data for each population

mtCR Statistic	Atlantic	east_Gulf	west_Gulf	Pacific
Samples	17	14	19	2
SNPs	5	8	8	1
Haplotypes	7	8	8	2
Mean number of pairwise differences	1.3317	2.1063	1.5422	1.0067
Nucleotide diversity	0.0026	0.0041	0.0030	0.0020
Haplotype diversity	0.8382	0.8242	0.8246	1.0000

Discussion/conclusion

Population structure

The nuclear data for *S. dumeril* in the western North Atlantic has a very clear signal of structure with the largest difference between the Atlantic and Gulf, corresponding to the known faunal break for multiple taxa along southern Florida (Neigel 2009) such as bonnethead (Fields et al. 2016; Portnoy et al. 2015), blacknose sharks (Portnoy et al. 2014), and blacktip sharks (Swift et al. 2023). Within the Gulf of Mexico, significant population structure was detected as well, aligning with the distribution break seen along the Mississippi Canyon (Driggers et al. 2018); however, no evidence was found to indicate cryptic speciation in the genetic data. Results obtained from the maternally inherited mtCR did not agree with the results obtained from nuclear data, since the mtCR indicated the Atlantic and eastern Gulf formed a group which differed from the western Gulf. The selected demographic model indicated that the split between the Atlantic and the Gulf occurred prior to the split within the Gulf, and there were low levels of historic gene flow between all adjacent populations since the last split. Taken together, the data seem to indicate

Table 4 Diversity characteristics of the ddRAD data for each population by dataset including the number of polymorphic sites (n), expected heterozygosity (H_e), and rarefied allelic richness (A_r)

	Neutral			*Outlier*			*Environmental*		
Population	n	H_e	A_r	n	H_e	A_r	n	H_e	A_r
Atlantic	5,853	0.287	2.568	27	0.469	3.14	825	0.510	3.494
east Gulf	6,431	0.295	2.623	27	0.435	2.776	848	0.504	3.511
west Gulf	6,180	0.288	2.706	24	0.304	3.211	822	0.494	3.623
Friedman's p-value		7.74E − 16	< 2.2E − 16		0.005	0.151		0.067	0.008

The p-value from Friedman's test for each measure is also presented

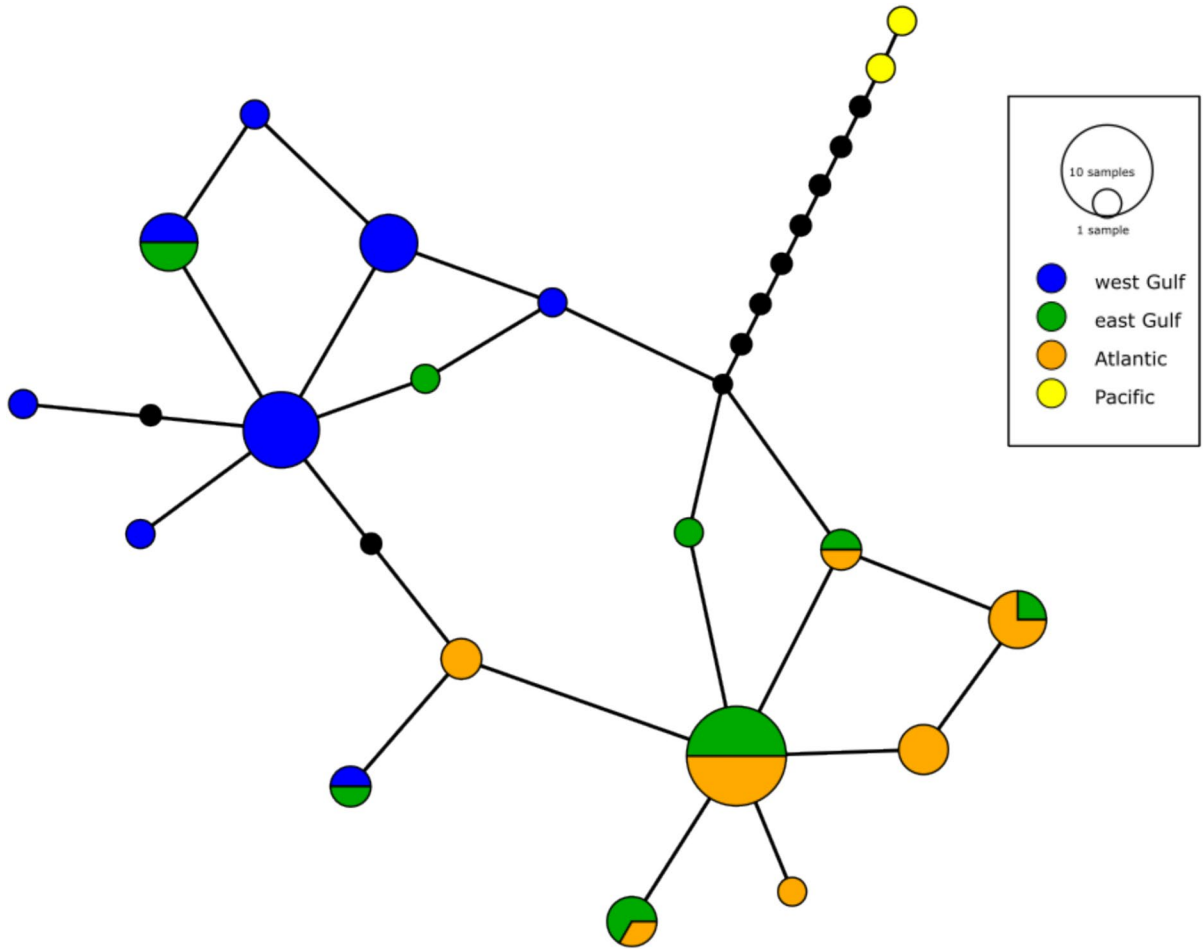

Fig. 4 Haplotype network of the mitochondrial control region (mtCR) color-coded by *k*-means clustering. The sizes denote the number of haplotypes ranging from 1 to 12

that the incongruence between the results of nuclear and mtCR data may be due to historical gene flow which was limited enough to prevent homogenization between the eastern Gulf and Atlantic but not to the degree that would prevent mitochondrial replacement.

Long-term spatial isolation results in the accumulation of genetic differences (Wright 1931), which leads to the divergence of the populations. Migration facilitates admixture thus allowing alleles to freely mix. Depending on the scenario of mixing, alleles once abundant in one population may become rare (Wolf et al. 2001; Fitzpatrick et al. 2020) and, therefore, more frequently lost through genetic drift (Hartl and Clark 2007). The speed at which this happens for mtCR can be greater since it is only maternally inherited and single-copy and, therefore, has a smaller effective population size (Buonaccorsi et al. 2001). The demographic modeling suggests that at the time of the Gulf split, the effective population size of the Eastern Gulf was small, and migration continued between the Atlantic and Gulf (Table 6). This could have led to mitochondrial introgression from the Atlantic to the eastern Gulf, driving the contemporary incongruence between the nuclear and mitochondrial signals.

Mitochondrial introgression has been seen between many fish species such as dusky and Galapagos sharks (*Carcharhinus obscurus* and *C. galapagensis*; Corrigan et al. 2017), tunas (*Thunnus alalunga* into *T. thynnus*, Bremer et al. 2005; *T. alalunga* into *T. orientalis*, Chow and Kishino 1995), and common shiner into striped shiner (*Luxilus cornutus* into

Table 6 The results from the demographic modeling including the point estimate, the Godambe Information Matrix value, and the conversion of the MOMENTS point estimates, which included a theta value of 8.23, to physical units using a mutation rate of 7.5E − 8 and a generation time of 14.5 years

Variable	Point estimate	GIM	Estimated value	Lower CI	Upper CI
Ancestral N_e	-	9.09	14.29	0.00	32.11
Atlantic N_E at $T1$	1.86	0.29	26.62	18.59	34.66
Atlantic N_e	191.21	10.26	2732.03	2444.70	3019.37
Gulf N_e at $T1$	1.93	0.23	27.58	21.09	34.07
Gulf N_e at $T2$	1.21	0.18	17.34	12.44	22.25
eastern Gulf N_e at $T1$	0.94	0.31	13.42	4.70	22.15
eastern Gulf N_e	6644.28	2832.32	94,933.86	15,615.84	174,251.88
western Gulf N_e at $T1$	14.65	0.07	209.35	207.31	211.40
western Gulf N_e	267.66	13.69	3824.30	3440.86	4207.75
Migration between Atl and the Gulf	0.03	0.00	0.00	0.00	0.00
Migration between Atl and east Gulf	28.81	3.05	1.01	0.80	1.22
Migration between east Gulf and west Gulf	57.15	3.15	2.00	1.78	2.22
Split of the Atlantic and the Gulf ($T1+T2$)	34.27	0.89	14,200.68	13,791.02	14,610.35
Split in the Gulf ($T2$)	24.44	0.39	10,127.79	9807.52	10,448.07

Long-term effective size estimates (N_e) are shown for a hypothetical ancestral population and for each current population, the western Gulf, the eastern Gulf, and the Atlantic (Atl) currently and a time just post-split. Long-term migration rates (m) are also shown between neighboring populations as are split times (T)

L. chrysocephalus, Duvernell and Aspinwall 1995). Intraspecies introgression is also possible within a species such as in the case of farmed European Atlantic salmon (*Salmo salar*) breeding with wild North American Atlantic salmon (Bradbury et al. 2022). While the incongruence between patterns recovered from mtCR and nuclear markers is common in marine species (Wallis et al. 2017), within elasmobranchs, results based on mtCR data typically show more structure than those based on nuclear data. This has been attributed to the philopatric behavior of females to nursery grounds/regions (Chapman et al. 2015) and male-mediated gene flow (e.g., Keeney et al. 2005; Portnoy et al. 2010; Karl et al. 2011). By contrast, the nuclear data in this study are more structured than the mtCR results but rather than being driven by behavior; this appears related to the demographic history of *S. dumeril*.

This study found no genetic evidence of more than one species within the sample regions as hypothesized by Driggers et al. (2018). While population differentiation was large enough to detect, the differences between the *S. dumeril* groups were tenfold less than those between the *S. dumeril* groups and their sister taxa, *S. californica* (Hebert et al. 2004). The results do not discount the possibility of multiple species in the Gulf as samples were not collected from Mexican waters (e.g., Castro-Aguirre et al. 2006), but the low F'_{ST} between *S. dumeril* and *S. califonica* relative to what is seen in some sympatric species (e.g., *Sphyrna lewini* and *S. gilberti* $F_{ST}=0.876$, Barker et al. 2019; *Cactoblastis cactorum* and *C. doddi* $F_{ST}=0.695$, Poveda-Martínez et al. 2022) does suggest an investigation into the classification of these two species may be warranted since geographic isolation and subsequent genetic drift alone do not guarantee speciation (Sobel et al. 2010). This investigation would need to consider phenotype as there are distinctive morphological traits between *S. dumeril* and *S. californica* (Compagno 1984).

Non-neutral loci

Driggers et al. (2018) found distinct differences in the depths occupied by *S. dumeril* in the Atlantic and the Gulf. In this study, sea surface temperature and two measures of nitrate concentration were associated with the genetic data rather than depth. However, depth was correlated with SST at these sampling locations ($r=0.76$) and was significantly associated

with the genetic data if it was the only factor in the RDA. Therefore, the distributional patterns seen by Driggers et al. (2018) may be due to the correlation of depth with other environmental factors identified here. Similarly, significant environmental factors identified using RDA here may also be serving as a proxy for variables that were not measured and therefore not tested. While patterns of variation do differ between the neutral and non-neutral, the geographic location of the samples dominates those patterns (Fig. 3).

While sea surface temperature and nitrate values were correlated with allele frequencies at a small subset of loci, the question remains whether this association is biologically meaningful as *S. dumeril* is a benthic species, often found at depths below the mixed layer. Nitrate is a limiting nutrient for primary productivity in marine systems (Redfield 1934), with coastal sources coming from runoff and upwelling. Upwelling can lead to cooler SST and mixing while river discharge can increase stratification and affect SST based on the river's characteristics (Anglès et al. 2019). The effects of upwelling and riverine input vary among the three distinct regions which correspond with the populations of angel sharks found in this study. Within the Atlantic, summer upwelling brings cold water and nutrients up along the shelf and to the surface of the water (Murphey et al. 2021). This is in contrast to rainfall, which is typically discharged more in winter and spring, leading to warmer freshwater and a more stratified water column (Roarty et al. 2020). During the summer, northerly winds lead to an easterly current in the northern Gulf, leading to upwelling along the western Gulf. These currents also move the Mississippi River discharge to the east until it is entrained in mesoscale eddies over the De Soto Canyon region where it is moved offshore, preventing it from continuing into the eastern Gulf and onto the West Florida Shelf (Schiller et al. 2011). In the Fall, the winds shift to increase the upwelling in the eastern Gulf and the Mississippi River input is entrained west, flowing along the shelf (Anglès et al. 2019). In this way, the western Gulf and Atlantic are more similar with summer upwelling and riverine influence in the winter and spring, while the eastern Gulf experiences upwelling in the winter and little riverine influence. Seasonal shifts in productivity would have an impact on energetics for all organisms, affecting processes like reproduction, growth, and movement. Given that the amount, type, and quality of prey available to angel sharks likely differ with environmental conditions, selection could be acting upon angel sharks to optimize their life history to make the best use of available resources in time and space. While this is an appealing idea, further research would be required to elucidate the exact mechanisms behind the sorting of regional adaptive variation.

Evolutionary history of *S. dumeril*

According to fossil records, *Squatina* evolved between 114 and 157.6 Mya in areas that are now part of Europe (Klug and Kriwet 2013). During this time frame, Europe was located in a shallow sea between North America and Asia, potentially allowing the dispersal of angel sharks among multiple continents and suggesting the ancestor to *S. dumeril* and *S. californica* was likely of European origin. Phylogenetic analyses of angel sharks suggest that *S. dumeril* and *S. californica* are sister species (Stelbrink et al. 2010; Acero et al. 2016; Cañedo-Apolaya et al. 2021; Cañedo-Apolya et al. 2021), and their divergence is thought to have occurred because of the rise of the Isthmus of Panama. Two separate molecular analyses, using fossil records for calibrations, have estimated that the split between *S. californica* and *S. dumeril* occurred in the late Miocene (3.58 to 8.64 Mya, Stelbrink et al. 2010) which is during the time frame of the rise of the Isthmus of Panama (2.8 to 8 Mya, McGirr et al. 2021; O'Dea et al. 2016).

This study provides further information on evolution in angel sharks by providing a hypothesis of what may have occurred to *S. dumeril* after the split from *S. californica*. A rudimentary rate of mutation was generated by mapping reads obtained from *S. dumeril* and the single *S. californica* to a published *S. squatina* genome (Genbank accession: GCA_031763465.1) using BWA (Li and Durbin 2009). The number of differences between *S. dumeril* and *S. californica* at putatively orthologous loci was then calculated as the average of the percent difference between each *S. dumeril* and *S. californica* (3.16% of 126,771 bp). Taking the estimated split between *S. dumeril* and *S. californica*, based upon previous molecular work using fossil calibrations, a divergence time of 6.11 Mya (Stelbrink

et al. 2010) could be used to set a nuclear mutation rate at 5.17×10^{-9} ($3.66\times10^{-9}-8.82\times10^{-9}$) substitutions/site/year. Using a generation rate of 14.5 years (Cailliet et al. 1992) and the point estimate, that becomes 7.50×10^{-8} substitutions/site/generation ($5.30\times10^{-8}-1.28\times10^{-7}$). This puts the point estimate of separation between the Atlantic and the Gulf *S. dumeril* around 14 kya and between the two Gulf populations around 10 kya (Table 6), both falling within the recession after the last glacial maximum (Martinson et al. 1987; Osman et al. 2021). After the Wisconsin glacial period, *S. dumeril* in the Atlantic likely shifted into northern waters to escape warming lower latitudes which has led to the Atlantic disjunction. During the glacial recession, pulses of freshwater discharged into the western North Atlantic along both the Atlantic and Gulf coasts from around 16 to 8.4 thousand years ago (Teller et al. 2002; Aharon 2003). In the Gulf, the Mississippi outflow, out of southeast Louisiana, was filled with pulses of cold, fresh glacial meltwater (Aharon 2003), likely leading to the bifurcation of the Gulf population. If both the Eastern Gulf and Atlantic populations were extended further south, or potentially displaced by glacial meltwater, gene flow could have been possible around the Florida peninsula. Glacial meltwater has also been hypothesized to have historically changed patterns of gene flow in other marine taxa in the northern Gulf including the purple marsh crab, *Sesarma reticulatum*, the blacknose shark, *Carcharhinus acronotus*, and species in the genus *Prionotus* (McClure and McEachran 1992; Felder and Staton 1994; Portnoy et al. 2014).

Some angel shark populations have been impacted by fishing practices (Gonzalez-Pestana et al. 2014; Ellis et al. 2021) as are many rays and ray-like sharks (Dulvy et al. 2014). While currently prohibited from being retained in the US, *S. dumeril* is currently caught as a bycatch (Vecchione 1987; Shepherd and Myers 2005). This potential source of indirect fishing mortality has had a significant effect on the abundance of other elasmobranchs including sawfish (Simpfendorfer 2000), barndoor skates (Casey and Myers 1998), and Bancroft's numbfish (Shepherd and Myers 2005); however, *S. dumeril* has not been shown to have any current population declines (Shepherd and Myers 2005). Through understanding population structure, the range and limitations of our knowledge (e.g., Northern Gulf population abundance) can be brought into perspective to aid in management decisions, setting monitoring boundaries, and setting direction for future research.

Acknowledgements The authors would like to thank J. Gartland (Virginia Institute of Marine Science) and Kristin Hannan (National Oceanic and Atmospheric Administration) as well as members of the Southeast Fisheries Science Center, Trawl and Plankton Branch for the collection of specimens in the northern Gulf of Mexico. The authors would like to thank the University of Kansas Biodiversity Institute (Andrew Bently) and the Scripps Marine Vertebrate Collection (Ben Frable) for the tissue samples. The authors would also like to thank the Marine Genomics Laboratory at Texas A&M—Corpus Christi for the valuable discussions. This is publication 39 of the Marine Genomics Laboratory and 131 of Genetic Studies in Fishes.

Author contribution WD, CJ, AF, and DP designed the experiment. WD, CJ, and AF collected the data. AF analyzed the data. AF led the manuscript preparation with contributions from DP. All authors reviewed, edited, and approved the manuscript for submission.

Funding David Portnoy has received research support from the Life Science Department at Texas A&M University at Corpus Christi.

Data availability Data from the Sanger sequencing is available on GenBank (Accession #PP952512-PP952563). Next Generation DNA sequencing data is available on GenBank (Accession #SRR30648325-SRR30648393). Tissue samples are available upon reasonable request from the Marine Genomics Lab via email to David.Portnoy@tamucc.edu or hri.marine.genomics.lab@gmail.com. The Variable Call–formatted data is available on GitHub (https://github.com/marinegenomicslab/Fields2024_Angel_Sharks.git).

Code availability All code used to filter and manipulate the filtered SNPs is available on GitHub (https://github.com/marinegenomicslab/Fields2024_Angel_Sharks.git).

Declarations

Ethics approval This research was carried out in accordance with all applicable institutional and national guidelines at the time that the study was conducted. Ethical review and approval was not required for the animal study because the trawls were conducted by the National Marine Fisheries Service, Southeast Fisheries Science Center, and Small Pelagics Trawl survey. The National Marine Fisheries Service does not have an Institutional Animal Care and Use Committee (IACUC) approval process for research on fishes. All work followed the American Fisheries Society policies on the Guidelines for Use of Fishes in Research (https://fisheries.org/docs/policy_useoffishes.pdf) and AVMA (American Veterinary Medical Association) Guidelines on Euthanasia (https://olaw.nih.gov/sites/default/files/Euthanasia2007.pdf).

Competing interests The authors declare no competing interests.

References

Acero PA, Tavera JJ, Anguila R, Hernández L (2016) A new southern Caribbean species of angel shark (Chondrichthyes, Squaliformes, Squatinidae), including phylogeny and tempo of diversification of American species. Copeia 104:577–585

Aharon P (2003) Meltwater flooding events in the Gulf of Mexico revisited: implications for rapid climate changes during the last deglaciation. Paleoceanography 18:1079

Anglès S, Jordi A, Henrichs DW, Campbell L (2019) Influence of coastal upwelling and river discharge on the phytoplankton community composition in the northwestern Gulf of Mexico. Prog Oceanogr 173:26–36

Barker AM, Adams DH, Driggers WB III, Frazier BS, Portnoy DS (2019) Hybridization between sympatric hammerhead sharks in the western North Atlantic Ocean. Biol Lett 15:20190004

Benjamini Y, Hochberg Y (1995) Controlling the false discovery rate: a practical and powerful approach to multiple testing. J R Stat Soc Series B Stat Method 57:289–300

Bosch S, Fernandez S (2021) sdmpredictors: species distribution modelling predictor datasets. R package version 0.2.10

Bradbury IR, Lehnert SJ, Kess T, Van Wyngaarden M, Duffy S, Messmer AM, Wringe B, Karoliussen S, Dempson JB, Fleming IA, Solberg MF, Glover KA, Bentzen P (2022) Genomic evidence of recent European introgression into North American farmed and wild Atlantic salmon. Evol Appl 15:1436–1448

Bremer JRA, Viñas J, Mejuto J, Ely B, Pla C (2005) Comparative phylogeography of Atlantic bluefin tuna and swordfish: the combined effects of vicariance, secondary contact, introgression, and population expansion on the regional phylogenies of two highly migratory pelagic fishes. Mol Phylogenet Evol 36:169–187

Buonaccorsi VP, McDowell JR, Graves JE (2001) Reconciling patterns of inter-ocean molecular variance from four classes of molecular markers in blue marlin (*Makaira nigricans*). Mol Ecol 10:1179–1196

Cadrin SX, Kerr LA, Mariani S (2014) Stock identification methods: applications in fishery science. Academic Press, Amsterdam

Cailliet GM, Mollet HF, Pittenger GG, Bedford D, Natanson LJ (1992) Growth and demography of the Pacific angel shark (*Squatina californica*), based upon tag returns off California. Aust J Mar Freshw Res 43:1313–1330

Cañedo-Apolaya RM, Ortiz-Alvarez C, Alfaro-Cordova E, Alfaro-Shigueto J, Velez-Zuazo X, Mangel JC, Siccha-Ramirez R, Yamashiro C, Ramirez JL (2021) Species delimitation of southeast Pacific angel sharks (Squatina spp.) reveals hidden diversity through DNA barcoding. Diversity 13:177

Casey JM, Myers RA (1998) Near extinction of a large, widely distributed fish. Science 281:690–692

Castro-Aguirre JL, Espinosa Pérez H, Huidobro Campos L (2006) Dos nuevas especies del género Squatina (Chondrichthyes: Squatinidae) del Golfo de México. Rev Biol Trop 54:1031–1040

Catchen J, Hohenlohe PA, Bassham S, Amores A, Cresko WA (2013) Stacks: an analysis tool set for population genomics. Mol Ecol 22:3124–3140

Chapman DD, Feldheim KA, Papastamatiou YP, Hueter RE (2015) There and back again: a review of residency and return migrations in sharks, with implications for population structure and management. Ann Rev Mar Sci 7:547–570

Chow S, Kishino H (1995) Phylogenetic relationships between tuna species of the genus *Thunnus* (Scombridae: Teleostei): inconsistent implications from morphology, nuclear and mitochondrial genomes. J Mol Evol 41:741–748

Clement M, Snell Q, Walke P, Posada D, Crandall K (2002) TCS: estimating gene genealogies. Proceedings of the 16th international symposium on parallel and distributed processing. International 2:184

Coffman AJ, Hsieh PH, Gravel S, Gutenkunst RN (2016) Computationally efficient composite likelihood statistics for demographic inference. Mol Biol Evol 33:591–593

Compagno LJV (1984) FAO species catalogue. Vol. 4. Sharks of the world. An annotated and illustrated catalogue of shark species known to date. Part 1. Hexanchiformes to Lamniformes. Rome: FAO, United Nations.

Corrigan S, Delser PM, Eddy C, Duffy C, Yang L, Li C, Bazinet AL, Mona S, Naylor GJ (2017) Historical introgression drives pervasive mitochondrial admixture between two species of pelagic sharks. Mol Phylogenet Evol 110:122–126

Danacek P, Auton A, Abecasis G, Albers CA, Banks E, DePristo MA, Handsaker R, Lunter G, Marth G, Sherry ST, McVean G, Durbin R, Group GPA (2011) The variant call format and VCFtools. Bioinformatics 27:2156–2158

Darriba D, Taboada GL, Doallo R, Posada D (2012) jModelTest 2: more models, new heuristics and parallel computing. Nat Methods 9:772

de Villwock ML, Vooren CM (2003) Catch and effort of demersal elasmobranchs in south Brazil from 1975 to 1997. Frente Marit 19:217–231

Driggers WB III, Campbell MD, Hanisko DS, Hannan KM, Hoffmayer ER, Jones CM, Pollack AG, Portnoy DS (2018) Distribution of angel sharks (Squatinidae) in United States waters of the western North Atlantic Ocean. Fish Bull 116:337–347

Dulvy NK, Fowler SL, Musick JA, Cavanagh RD, Kyne PM, Harrison LR, Carlson JK, Davidson LN, Fordham SV, Francis MP (2014) Extinction risk and conservation of the world's sharks and rays. elife 3:e00590

Duvernell DD, Aspinwall N (1995) Introgression of *Luxilus cornutus* mtDNA into allopatric populations of *Luxilus chrysocephalus* (Teleostei: Cyprinidae) in Missouri and Arkansas. Mol Ecol 4:173–182

Ellis JR, Barker J, Phillips SRM, Meyers EKM, Heupel M (2021) Angel sharks (Squatinidae): a review of biological knowledge and exploitation. J Fish Biol 98:592–621

Excoffier L, Lischer HEL (2010) Arlequin suite ver 3.5: a new series of programs to perform population genetics analyses under Linux and Windows. Mol Ecol Res 10:564–567

Felder DL, Staton JL (1994) Genetic differentiation in trans-Floridian species complexes of *Sesarma* and *Uca* (Decapoda: Brachyura). J Crustacean Biol 14:191–209

Ferretti F, Worm B, Britten GL, Heithaus MR, Lotze HK (2010) Patterns and ecosystem consequences of shark declines in the ocean. Ecol Lett 13:1055–1071

Fields AT, Feldheim KA, Gelsleichter J, Pfoertner C, Chapman DD (2016) Population structure and cryptic speciation in bonnethead sharks *Sphyrna tiburo* in the south-eastern U.S.A. and Caribbean. J Fish Biol 89:2219–2233

Fischer MC, Foll M, Excoffier L, Heckel G (2011) Enhanced AFLP genome scans detect local adaptation in high-altitude populations of a small rodent (*Microtus arvalis*). Mol Ecol 20:1450–1462

Fitzpatrick SW, Bradburd GS, Kremer CT, Salerno PE, Angeloni LM, Funk WC (2020) Genomic and fitness consequences of genetic rescue in wild populations. Curr Biol 30:517–522

Foll M, Gaggiotti O (2008) A genome-scan method to identify selected loci appropriate for both dominant and codominant markers: a Bayesian perspective. Genetics 180:977–993

Fricke R, Eschmeyer WN, van der Laan R (2024) Eschmeyer's catalog of fishes: genera, species, references. http://researcharchive.calacademy.org/research/ichthyology/catalog/fishcatmain.asp. Electronic version accessed 10 May 2024.

Funk WC, McKay JK, Hohenlohe PA, Allendorf FW (2012) Harnessing genomics for delineating conservation units. Trends Ecol Evol 27:89–496

Gaida IH (1997) Population structure of the Pacific angel shark, *Squatina californica* (Squatiniformes: Squatinidae), around the California Channel Islands. Copeia 1997:738–744

Gonzalez-Pestana A, Kouri C, Velez-Zuazo X (2014) Shark fisheries in the Southeast Pacific: a 61-year analysis from Peru. F1000Research 3:164

Goudet J, Jombart T (2020) hierfstat: estimation and tests of hierarchical F-Statistics. R package version 0.5-7

Gruber B, Unmack PJ, Berry OF, Georges A (2018) Dartr: an R package to facilitate analysis of SNP data generated from reduced representation genome sequencing. Mol Ecol Res 18:691–699

Gutenkunst RN, Hernandez RD, Williamson SH, Bustamante CD (2009) Inferring the joint demographic history of multiple populations from multidimensional SNP frequency data. PLoS Genet 5:e1000695

Hall TA (1999) BioEdit: a user-friendly biological sequence alignment editor and analysis program for Windows 95/98/NT. Nucl Acids Symp Ser 41:95–98

Hartl DL, Clark AG (2007) Principles of population genetics. Oxford University Press, New York, New York

Hebert PDN, Stoeckle MY, Zemlak TS, Francis CM (2004) Identification of birds through DNA barcodes. PLoS Biol 2:e312

Hothorn T, Hornik K, van de Wiel MA, Zeileis A (2006) A LEGO system for conditional inference. Amer Stat 60:257–263

Jombart T (2008) Adegenet: a R package for the multivariate analysis of genetic markers. Bioinformatics 24:1403–1405

Jouganous J, Long W, Ragsdale AP, Gravel S (2017) Inferring the joint demographic history of multiple populations: beyond the diffusion approximation. Genetics 206:1549–1567

Karl SA, Castro ALF, Lopez JA, Charvet P, Burgess GH (2011) Phylogeography and conservation of the bull shark (*Carcharhinus leucas*) inferred from mitochondrial and microsatellite DNA. Conserv Genet 12:371–382

Keeney DB, Heupel MR, Hueter RE, Heist EJ (2005) Microsatellite and mitochondrial DNA analyses of the genetic structure of blacktip shark (*Carcharhinus limbatus*) nurseries in the northwestern Atlantic, Gulf of Mexico, and Caribbean Sea. Mol Ecol 14:1911–1923

Klug S, Kriwet J (2013) Node age estimations and the origin of angel sharks, Squatiniformes (Neoselachii, Squalomorphii). J Syst Palaeontol 11:91–110

Last PR, White WT (2008) Three new angel sharks (Chondrichthyes: Squatinidae) from the Indo-Australian region. Zootaxa 1734:1–26

Lawson JM, Pollom RA, Gordon CA, Barker J, Meyers EKM, Zidowitz H, Ellis JR, Bartolí Á, Morey G, Fowler SL, Alvarado DJ, Fordham SV, Sharp R, Hood AR, Dulvy NK (2020) Extinction risk and conservation of critically endangered angel sharks in the Eastern Atlantic and Mediterranean Sea. ICES J Mar Sci 77:12–29

Leet W, Dewees C, Klingbeil R, Larson E (2001) California's marine living resources: a status report. Sacramento, California, The Resources Agency, The California Department of Fish and Game

Leigh JW, Bryant D (2015) PopART: full-feature software for haplotype network construction. Methods Ecol Evol 6:1110–1116

Li H, Durbin R (2009) Fast and accurate short read alignment with Burrows-Wheeler transform. Bioinformatics 25:1754–1760

Long DJ, Ebert DA, Tavera J, Acero PA, Robertson DR (2021) *Squatina mapama* n. sp., a new cryptic species of angel shark (Elasmobranchii: Squatinidae) from the southwestern Caribbean Sea. J Ocean Sci Found 38:113–130

Martinson DG, Pisias NG, Hays JD, Imbrie J, Moore TC, Shackleton NJ (1987) Age dating and the orbital theory of the ice ages: development of a high-resolution 0 to 300,000-year chronostratigraphy. Quat Res 27:1–29

McClure MR, McEachran JD (1992) Hybridization between *Prionotus alatus* and *P. paralatus* in the northern Gulf of Mexico (Pisces: Triglidae). Copeia 1992:1039–1046

McGirr R, Seton M, Williams S (2021) Kinematic and geodynamic evolution of the Isthmus of Panama region: implications for Central American Seaway closure. GSA Bull 133:867–884

McMillan HA (2009) Phylogeographic distribution and biogeography of the Atlantic angel shark, *Squatina dumeril*, L. 1818. Thesis, University of Aberdeen

Meirmans PG, Hedrick PW (2011) Assessing population structure: F_{ST} and related measures. Mol Ecol Res 11:5–18

Murphy SC, Nazzaro LJ, Simkins J, Oliver MJ, Kohut J, Crowley M, Miles TN (2021) Persistent upwelling in the Mid-Atlantic Bight detected using gap-filled, high-resolution satellite SST. Remote Sens Environ 262:112487

Neigel JE (2009) Population genetics and biogeography of the Gulf of Mexico. In: Feldr DL, Camp DK (eds) Gulf of Mexico – origins, waters, and biota: Biodiversity. Texas A&M University Press, College Station, TX, pp 1353–1369

Noskova E, Ulyantsev V, Koepfli KP, O'Brien SJ, Dobrynin P (2020) GADMA: genetic algorithm for inferring demographic history of multiple populations from allele frequency spectrum data. GigaScience 9:giaa005

O'Dea A, Lessios HA, Coates AG, Eytan RI, Restrepo-Moreno SA, Cione AL, Laurel S, Collins de Queiroz A, Farris DW, Norris RD, Stallard RF, Woodburne MO, Aguilera O, Aubry M-P, Berggren WA, Budd AF, Cozzuol MA, Coppard SE, Duque-Caro H, Finnegan S, Gasparini GM, Grossman EL, Johnson KG, Keigwin LD, Knowlton N, Leigh EG, Leonard-Pingel JS, Marko PB, Pyenson ND, Rachello-Dolmen PG, Soibelzon E, Soibelzon L, Todd JA, Vermeij GJ, Jackson JB (2016) Formation of the Isthmus of Panama. Sci Adv 2:e1600883

O'Leary SJ, Puritz JB, Willis SC, Hollenbeck CM, Portnoy DS (2018) These aren't the loci you're looking for: principles of effective SNP filtering for molecular ecologists. Mol Ecol 27:3193–3206

Oksanen J, Blanchet FG, Friendly M, Kindt R, Legendre P, McGlinn D, Minchin PR, O'Hara RB, Simpson GL, Solymos P, Stevens MHH, Szoecs E, Wagner H (2019) Vegan: community ecology package. R package version v2.5–7

Osman MB, Tierney JE, Zhu J, Tardif R, Hakim GJ, King J, Poulsen CJ (2021) Globally resolved surface temperatures since the Last Glacial Maximum. Nature 599:239–244

Overcast I (2022) easySFS, GitHub repository. Available at: https://github.com/isaacovercast/easySFS

Peterson BK, Weber JN, Kay EH, Fisher HS, Hoekstra HH (2012) Double digest RADseq: an inexpensive method for de novo SNP discovery and genotyping in model and non-model species. PLoS ONE 7:e37135

Portik DM, Leaché AD, Rivera D, Barej MF, Burger M, Hirschfeld M, Rödel M, Blackburn DC, Fujita MK (2017) Evaluating mechanisms ofdiversification in a Guineo-Congolian tropical forest frog using demographicmodel selection. Mol Ecol 26:5245–5263

Portnoy DS, McDowell JR, Heist EJ, Musick JA, Graves JE (2010) World phylogeography and male-mediated gene flow in the sandbar shark, *Carcharhinus plumbeus*. Mol Ecol 19:1994–2010

Portnoy DS, Hollenbeck CM, Belcher CN, Driggers WB III, Frazier BS, Gelsleichter J, Grubbs RD, Gold JR (2014) Contemporary population structure and post-glacial genetic demography in a migratory marine species, the blacknose shark, *Carcharhinus acronotus*. Mol Ecol 23:5480–5495

Portnoy DS, Puritz JB, Hollenbeck CM, Gelsleichter J, Chapman D, Gold JR (2015) Selection and sex-biased dispersal in a coastal shark: the influence of philopatry on adaptive variation. Mol Ecol 24:5877–5885

Poveda-Martínez D, Varone L, Corona MF, Hight S, Logarzo G, Hasson E (2022) Spatial and host related genomic variation in partially sympatric cactophagous moth species. Mol Ecol 31:356–371

Puritz JB, Hollenbeck CM, Gold JR (2014) dDocent: a RADseq, variant-calling pipeline designed for population genomics of non-model organisms. PeerJ 2:e431

R Core Team (2019) R: a language and environment for statistical computing. R Foundation for statistical computing, Vienna, Austria. https://www.R-project.org/

Raoult V, Peddemors V, Williamson JE (2017) Biology of angel sharks (*Squatina* sp.) and sawsharks (*Pristiophorus* sp.) caught in south-eastern Australian trawl fisheries and the New South Wales shark-meshing (bather-protection) program. Mar Freshw Res 68:207–212

Redfield AC (1934) On the proportions of organic derivatives in sea water and their relation to the composition of plankton. In: Daniel RJ (ed) James Johnstone memorial volume. University Press of Liverpool, Liverpool, pp 177–192

Roarty H, Glenn S, Brodie J, Nazzaro L, Smith M, Handel E, Kohut J, Updyke T, Atkinson L, Boicourt W, Brown W, Seim H, Muglia M, Wang H, Gong D (2020) Annual and seasonal surface circulation over the Mid-Atlantic Bight continental shelf derived from a decade of high frequency radar observations. J Geophys Res Oceans 125:e2020JC016368

Sbrocco EJ, Barber PH (2013) MARSPEC: ocean climate layers for marine spatial ecology. Ecology 94:979

Scandol J, Rowling K, Graham K (2008) Angel sharks. In Status of fisheries resources in NSW 2006/07. Cronulla, New South Wales: NSW Department of Primary Industries, Cronulla

Schiller RV, Kourafalou VH, Hogan P, Walker ND (2011) The dynamics of the Mississippi River plume: impact of topography, wind and offshore forcing on the fate of plume waters. J Geophys Res 116:C06029

Shepherd TD, Myers RA (2005) Direct and indirect fishery effects on small coastal elasmobranchs in the northern Gulf of Mexico. Ecol Lett 8:1095–1104

Sievers F, Wilm A, Dineen D, Gibson TJ, Karplus K, Li W, Lopez R, McWilliam H, Remmert M, Söding J, Thompson JD, Higgins DG (2011) Fast, scalable generation of high-quality protein multiple sequence alignments using Clustal Omega. Mol Syst Biol 7:539

Simpfendorfer CA (2000) Predicting population recovery rates for endangered western Atlantic sawfishes using demographic analysis. Environ Biol Fishes 58:371–377

Sinnott RW (1984) Virtues of the Haversine. Sky and Telescope 68:159

Sobel JM, Chen GF, Watt LR, Schemske DW (2010) The biology of speciation. Evol 64:295–315

Stelbrink B, von Rintelen T, Cliff G, Kriwet J (2010) Molecular systematics and global phylogeography of angel sharks (genus *Squatina*). Mol Phylogenet Evol 54:395–404

Swift DG, O'Leary SJ, Grubbs RD, Frazier BS, Fields AT, Gardiner JM, Drymon JM, Bethea DM, Wiley TR, Portnoy DS (2023) Philopatry influences the genetic population structure of the blacktip shark (*Carcharhinus limbatus*) at multiple spatial scales. Mol Ecol 32:4953–4970

Tamura K, Nei M (1993) Estimation of the number of nucleotide substitutions in the control region of mitochondrial DNA in humans and chimpanzees. Mol Biol Evol 10:512–526

Teller JT, Leverington DW, Mann JD (2002) Freshwater outbursts to the oceans from glacial Lake Agassiz and their role in climate change during the last deglaciation. Quat Sci Rev 21:879–887

Tyberghein L, Verbruggen H, Pauly K, Troupin C, Mineur F, De Clerck O (2012) Bio-ORACLE: a global environmental dataset for marine species distribution modelling. Glob Ecol Biogeogr 21:272–281

Vaz DFB, De Carvalho MR (2018) New species of Squatina (Squatiniformes: Squatinidae) from Brazil, with comments on the taxonomy of angel sharks from the central and northwestern Atlantic. Copeia 106:144–160

Vecchione M (1987) Commercial fishing for gulf butterfish, *Peprilus burti*. Mar Fish Rev 49:14–22

Wallis GP, Cameron-Christie SR, Kennedy HL, Palmer G, Sanders TR, Winter DJ (2017) Interspecific hybridization causes long-term phylogenetic discordance between nuclear and mitochondrial genomes in freshwater fishes. Mol Ecol 26:3116–3127

Weigmann S, Vaz DFB, Akhilesh KV, Leeney RH, Naylor GJP (2023) Revision of the western Indian Ocean angel sharks, genus *Squatina* (Squatiniformes, Squatinidae), with description of a new species and redescription of the African angel shark *Squatina africana* Regan, 1908. Biology 12:975

Whitlock MC, Lotterhos KE (2015) Reliable detection of loci responsible for local adaptation: inference of a null model through trimming the distribution of F_{ST}. Am Nat 186:S24–S36

Willis SC, Hollenbeck CM, Puritz JB, Gold JR, Portnoy DS (2017) Haplotyping RAD loci: an efficient method to filter paralogs and account for physical linkage. Mol Ecol Res 17:955–965

Wolf DE, Takebayashi N, Rieseberg LH (2001) Predicting the risk of extinction through hybridization. Conserv Biol 15:1039–1053

Worm B, Davis B, Kettemer L, Ward-Paige CA, Chapman D, Heithaus MR, Kessel ST, Gruber SH (2013) Global catches, exploitation rates, and rebuilding options for sharks. Mar Policy 40:194–204

Wright S (1931) Evolution in Mendelian populations. Genetics 16:97–159

Zuur AF, Ieno EN, Elphick CS (2010) A protocol for data exploration to avoid common statistical problems. Methods Ecol Evol 1:3–14